A Scalable Helmholtz Solver Combining the Shifted Laplace Preconditioner With Multigrid Deflation

A.H. Sheikh, D. Lahaye, C. Vuik

January 14, 2011

Abstract

We show that a scalable Helmholtz solver can be obtained by combining the shifted Laplace preconditioner with deflation. The term scalable here refers to the part that the number of iterations does not depend upon parameters. Our solver exploits the fact that the shifted Laplace preconditioner brings most operator eigenvalues in a location favorable for the convergence of Krylov subspace methods. The few remaining eigenvalues that prevent wavenumber independent convergence can subsequently be removed using deflation. We quantify these claims by deriving expressions for the eigenvalues of deflated preconditioner using two-grid Fourier analysis. Numerical test with constant and piecewise constant wavenumbers demonstrate that our solver is indeed scalable.

1 Introduction

The aim in this work is to develop high performance iterative solution algorithm for solving the discrete Helmholtz equation modeling wave propagation on large scale. Ingredients in our work are the shifted Laplace preconditioner and deflation. The development of the shifted Laplace preconditioner for the Helmholtz equation was a breakthrough in the development of efficient solution techniques for the Helmholtz equation. The distinct feature of this preconditioner is the introduction of a complex shift, effective introducing damping of wave propagation in the approximate solve. This preconditioner was extensively studied in [5] and applied in a number of different contexts [8, 6, 2]. Although performant, the resulting algorithm is not truly scalable. The bigger the wavenumber, the more spectrum scatters away from one, hampering the convergence. Idea of projection has been used since long to deflate unfavorable eigenvalues. By inducting eigenvectors corresponding to unwanted eigenvalues, better convergence for CG and GMRES has been seen [15] & [13]. For further see [4]. Recently, in [11], inspite of discarding, they presented FGMRES utilizing the harmonic Ritz vectors at restart. Idea is following [14]. Explicit projection of eigenvalues has been used in [17] & [8]. In later they have tested Helmholtz problem too. For further details, subsection (3.2) is referred. We provide a convergence analysis. We perform a Fourier two-grid analysis of one-dimensional model problem with Dirichlet boundary conditions discretized by a second order accurate finite difference scheme. The components analyzed are the shifted Laplace preconditioner used as smoother, full-weighting and linear interpolation intergrid transfer operators, and a Galerkin coarsening scheme. This Fourier analysis results in a closed form expression for the eigenvalues of the two-grid operator. This expressions shows that the spectrum is favourable for convergence of Krylov subspace methods. We apply the deflated shifted Laplace preconditioner to two-dimensional model problems method with constant and non-constant wave numbers and Sommerfeld boundary conditions discretized by second order accurate finite difference

scheme on uniform meshes. Numerical results show that the number of GMRES iterations is wavenumber independent.
This paper is structured as follows: In Section 2, we describe two Helmholtz problems with and without heterogeneity, domain and discretization of problems. In section 3, the multigrid deflation along with shifted Laplace preconditioner is discussed. Theoretical results from Fourier analysis of 1-D Helmholtz are presented in Section 4. In Section 5, supporting numerical results are showed and finally the conclusions are given in Section 6

2 Problem Formulation

The Helmholtz equation for the unknown field $u(x, y)$ on a two-dimensional domain Ω with boundary $\partial\Omega$ reads

$$-\Delta u - k^2 u = g\,, \tag{2.1}$$

where $k(x, y)$ the wave number and $g(x, y)$ the source function. The wavenumber k, the frequency f and angular frequency $\omega = 2\pi f$, the speed of propagation $c(x, y)$ and the wavelength $\lambda = \frac{c(x,y)}{f}$ are related by

$$k = \frac{2\pi}{\lambda} = \frac{\omega}{c}\,. \tag{2.2}$$

On the boundary $\partial\Omega$ we impose the first order Sommerfeld radiation boundary conditions

$$\frac{\partial u}{\partial n} - \imath k u = 0\,. \tag{2.3}$$

We will consider two model problems. In the first we set $\Omega = (0, 1) \times (0, 1)$, the wavenumber constant and source is defined as Dirac delta function g which is

$$g(x, y) = \delta(x - \frac{1}{2}, y - \frac{1}{2})\,. \tag{2.4}$$

As second problem we consider is the so-called wedge-problem introduced in [16] in which $\Omega = (0, 600) \times (0, 1000)$ is subdivided into three layers as shown in Figure 2. In each layer the velocity is constant and the constant is set as shown in this figure.

The finite difference discretization of the model problems on a mesh with meshwidth h in both x and y direction has the following stencil

$$[A_h] = \frac{1}{h^2}\begin{bmatrix} 0 & -1 & 0 \\ -1 & 4-\kappa^2 & -1 \\ 0 & -1 & 0 \end{bmatrix}, \tag{2.5}$$

where $\kappa = k\,h$, leads to a system of linear equations

$$A_h x_h = b_h, \tag{2.6}$$

where the discrete Helmholtz A_h is the sum of a stiffness matrix Δ_h and k^2 times the identify

$$A_h = -\Delta_h - k^2 I_h\,. \tag{2.7}$$

For the discretization scheme chosen the rule of thumb of using 'at least 10 nodes per wavelength' leads to the restriction

$$\kappa \approx \frac{2\pi}{10}\,. \tag{2.8}$$

The matrix A_h is complex-valued, sparse, symmetric and indefinite for sufficiently large wavenumber.

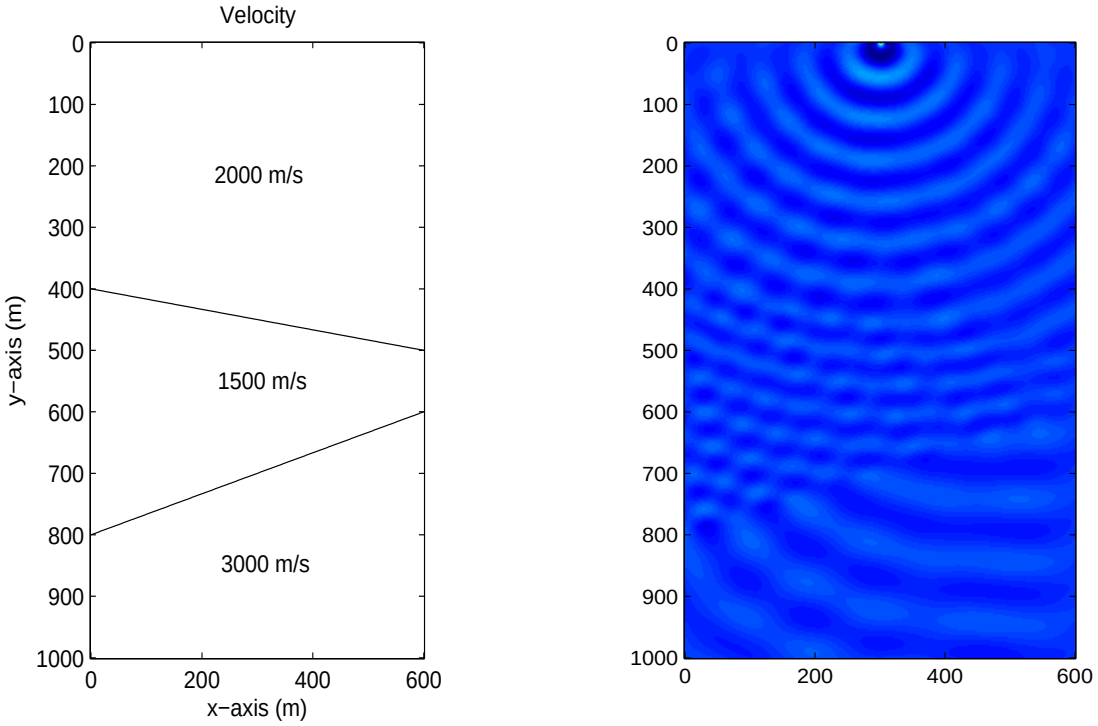

Figure 1: Left: Domain of wedge problem with actual parameters, Right: Real part of the solution.

3 Two-grid Deflated Shifted Laplace Preconditioner

The linear system (2.6) is complex valued, symmetric, non-Hermitian and sparse for all problems stated in Section (2). Solving this linear system necessarily requires the use of iterative solution techniques. GMRES and Bi-CGSTAB are choices for this system. Krylov subspace methods, in general, converge for system with favorable spectrum. Preconditioning is used to transform spectrum into favorable one. In this work we make use of the shifted Laplace preconditioner and deflation.

3.1 Shifted Laplace Preconditioner

This class of preconditioners for the Helmholtz equation contains the most effective preconditioner, *shifted Laplace preconditioners*. The idea started with the preconditioner obtained by discretizing Laplace operator $M = A$, which was used as preconditioner in [1]. Later an additional real term Shift was added into the Laplace operator, making this preconditioner resembling more the Helmholtz operator but with an opposite sign as investigated in [12]. Later Laplace operator with an imaginary shift was introduced in [5] and found to be more effective for the Helmholtz equation, and named complex shifted Laplace preconditioner (For details, see [9, 5]). A complex shift introduces damping and renders the preconditioned system amenable to approximate inversion by multigrid and MILU. This is developed by a discretization of the operator

$$M_{h,(\beta_1,\beta_2)} = -\Delta_h - (\beta_1 + \iota\beta_2)k^2 I_h, \qquad \beta_1, \beta_2 \in R \tag{3.1}$$

where β_1 and β_2 are real and complex shifts respectively. The geometric multigrid has been used to solve the shifted Laplace preconditioner [6, 5]. Recently an algebraic multigrid based shifted Laplace preconditioned has been presented in [2, 3]. The shifted Laplace preconditioner with both real and imaginary shifts is best when solved by multigrid. Since in this paper, for all results the preconditioner is solved by a direct solver therefore only an imaginary shift is used. For the notation, $M(0,0)$ is simply discretized Laplace preconditioner without any shift, $M(-1,0)$ is preconditioning matrix with real shift , and $M(0,1)$ is the complex shifted Laplace preconditioner. The spectral properties of the shifted Laplace operator are elaborated in [8] and it is showed that the spectrum of the discrete Helmholtz operator preconditioned by a shifted Laplacian is clustered near one, but some eigenvalues lie at $O(\epsilon/k^2)$. The eigenvalues are bounded above by one but the smallest eigenvalues rush to zero as k increases. With increase in wavenumber, iterative scheme encompass some very small eigenvalues, which cause slow convergence. In this paper, the small eigenvalues are handled by *deflation*.

3.2 Two-grid Deflation

Krylov subspace methods for linear systems are typically adversely affected by a few unfavorable eigenvalues of the coefficient matrix. Deflation is a technique to deal with those undesired eigenvalues. Deflation for SPD systems is used in [17] and [10] with Conjugate Gradient to improve the condition number. Various ideas such as sub-domain deflation are used in [10]. Later this idea was extended to non-symmetric systems in [10, 7]. The basic idea is to deflate the smallest eigenvalues to zero by choosing eigenvectors or approximate eigenvectors corresponding to those smallest eigenvalues as deflation vectors [10] and [17]. In [7], instead of deflating the small eigenvalues to zero, a deflation preconditioner is discussed which deflates the smallest eigenvalues of discretized preconditioned Helmholtz operator around zero to the maximum eigenvalue (in absolute value for a complex eigenvalue). Defining deflation for any matrix $Z \in R^{n\times k}$ of deflating vectors, the projection is defined as

$$P = I - QA \text{ with } Q = ZE^{-1}Z^T \text{ and } E = Z^TAZ\,, \tag{3.2}$$

where E is called the Galerkin or coarse matrix and Z the matrix, whose columns span the deflation subspace, is chosen such that E is non-singular. For A SPD, it is sufficient that $Rank(Z) = k$. Further properties of deflation space for an arbitrary Z are elaborated in detail in [17] and [7]. For the problems with large wavenumber k, the spectrum has more small eigenvalues, and a large deflation matrix Z will be needed to deflate these small eigenvalues. A large deflation matrix Z leads to large E, which can be impractical to solve by a direct solver. One may solve E then iteratively and its iterative solution may lead to scattering of very small eigenvalues. A tight stopping criteria can prevent this. An other idea of deflating eigenvalues to the maximum eigenvalue can be favorable. It is not theoretically established how to choose Z, but an optimal choice for matrix Z in Equation (3.2) is to set eigenvectors of the matrix as columns of deflation matrix Z. This is of course expensive in terms of memory. When choosing Z, one should take care that it should be sparse. In [7], piece-wise constant interpolation is used to construct Z, as in multigrid. We use multigrid-deflation vectors, which are very sparse and hence cheap to store and use.

In solving the model problems presented in Section 2 we will perform multigrid deflation. This means that we perform standard $h \to H = 2h$ coarsening in each coordinate direction and set the matrix Z in (3.2) equal to the coarse to fine grid interpolation operator I_H^h. With this choice the deflation operator denoted as $P_{h,H}$ coincides with the coarse grid correction operator in which the coarse grid operator is built by Galerkin coarsening, i.e.,

$$P_{h,H} = I_h - I_H^h(A_H)^{-1}I_h^H A_h \text{ with } A_H = I_h^H A_h I_H^h\,, \tag{3.3}$$

The Galerkin construction of A_H guarantees that the operator $P_{h,H}$ is a (real valued) projection. This coarse grid correction has to complemented with the action of a smoother S_h on the fine grid. As smoother, we choose the shifted Laplace operator splitting of A_h defined by (3.1), i.e., we set

$$S_{h,(\beta_1,\beta_2)} = I_h - M^{-1}_{h,(\beta_1,\beta_2)} A_h \,. \tag{3.4}$$

The combined operator resulting from one pre-smoothing set and a coarse grid correction step will be denoted as

$$B_{h,H,(\beta_1,\beta_2)} = P_{h,H} S_{h,(\beta_1,\beta_2)} \,. \tag{3.5}$$

Using this operator as a preconditioner for GMRES, results in a scalable solver in the sense that the number of iterations does not depend on the wavenumber.

4 Fourier Two-Grid Analysis

For an analysis of preconditioner, we consider the 1-D Helmholtz equation on the domain $\Omega = (0, 1)$ supplied with homogeneous Dirichlet boundary conditions. Assuming p to be a non-zero natural number, we discretize Ω by uniform mesh with $n = 2^p$ elements and with mesh width $h = 1/n$. Standard $h \to H = 2h$ coarsening of the fine mesh denoted by Ω^h will result in a coarse mesh denoted by Ω^H. Second order finite difference discretization on Ω^h with stencil

$$[A_h] = \frac{1}{h^2} \begin{bmatrix} -1 & 2-\kappa^2 & -1 \end{bmatrix} \tag{4.1}$$

results after elimination of the boundary conditions in the linear system

$$A_h x_h = b_h \tag{4.2}$$

of size $n-1$. The grid vectors

$$\phi^\ell_h = \sin(\ell\pi x) \text{ for } 1 \le \ell \le n-1 \tag{4.3}$$

are eigenvectors of A_h corresponding to the eigenvalues

$$\lambda^\ell(A_h) = \frac{1}{h^2}(2 - 2\cos(\ell\pi h) - \kappa^2) = \frac{1}{h^2}(2 - 2\,\mathrm{c}_\ell - \kappa^2) \,. \tag{4.4}$$

where

$$\mathrm{c}_\ell = \cos(\ell\pi h)$$

. To diagonalize the multigrid deflated shifted Laplace operator, we proceed in the standard way [18] and reorder the basis vectors according to

$$V_h = [\phi^1_h, \phi^{n-1}_h, \phi^2_h, \phi^{n-2}_h, ..., \phi^{n/2-1}_h, \phi^{n/2}_h] \tag{4.5}$$

This basis brings A_h into a block diagonal form that can be written as

$$A_h = \left[A^\ell_h\right]_{1 \le \ell \le n/2} \tag{4.6}$$

where for $1 \le \ell \le n/2 - 1$ A^ℓ_h is the 2×2 diagonal block

$$A^\ell_h = \begin{bmatrix} \frac{1}{h^2}(2 - 2\,\mathrm{c}_\ell - \kappa^2) & 0 \\ 0 & \frac{1}{h^2}(2 + 2\,\mathrm{c}_\ell - \kappa^2) \end{bmatrix} \tag{4.7}$$

and $A^{n/2}_h$ is the 1×1 block

$$A^{n/2}_h = \frac{2}{h^2} - k^2 \,. \tag{4.8}$$

In what follows we will diagonalize the smoother and coarse grid operator separately to be able to derive closed form expressions for the two-grid operator in a sequential stage.

4.1 Smoothing Analysis

The vectors (4.5) are eigenvectors of $M_{h,(\beta_1,\beta_2)}$ corresponding to the eigenvalues

$$\lambda_h^\ell(M_{h,(\beta_1,\beta_2)}) = \frac{1}{h^2}[2 - 2\,\mathrm{c}_\ell - (\beta_1 - \iota\beta_2)\kappa^2]\,. \tag{4.9}$$

The eigenvalues of the smoother (3.4) are therefore given by

$$\lambda^l(S_{h,(\beta_1,\beta_2)}) = 1 - \frac{2 - 2\,\mathrm{c}_\ell - \kappa^2}{2 - 2\,\mathrm{c}_\ell - (\beta_1 - \iota\beta_2)\kappa^2} \tag{4.10}$$

The diagonalization of $S_{h,(\beta_1,\beta_2)}$ in the basis (4.5) results in the 2×2 blocks

$$S^\ell_{h,(\beta_1,\beta_2)} = \begin{bmatrix} 1 - \frac{2-2\,\mathrm{c}_\ell-\kappa^2}{2-2\,\mathrm{c}_\ell-(\beta_1-\iota\beta_2)\kappa^2} & 0 \\ 0 & 1 - \frac{2+2\,\mathrm{c}_\ell-\kappa^2}{2+2\,\mathrm{c}_\ell-(\beta_1-\iota\beta_2)\kappa^2} \end{bmatrix} \tag{4.11}$$

for $1 \le \ell \le n/2 - 1$ and the 1×1 block

$$S^{n/2}_{h,(\beta_1,\beta_2)} = 1 - \frac{2 - \kappa^2}{2 - (\beta_1 - \iota\beta_2)\kappa^2}\,. \tag{4.12}$$

4.2 Coarse Grid Correction Analysis

As restriction operator I_h^H we will use the full weighting operator with stencil

$$[I_h^H] = \begin{bmatrix} \frac{1}{4} & \frac{1}{2} & \frac{1}{4} \end{bmatrix} \tag{4.13}$$

and as prolongation operator I_H^h linear interpolation. Given the fact that the basis (4.5) diagonalizes the linear interpolation operator $I_H^h \in \mathbb{R}^{n\times(\frac{n}{2}-1)}$ into blocks

$$(I_H^h)^\ell = \begin{bmatrix} \frac{1}{2}(1 + \mathrm{c}_\ell) & -\frac{1}{2}(1 - \mathrm{c}_\ell) \end{bmatrix} \tag{4.14}$$

for $1 \le \ell \le n/2 - 1$ and $(I_H^h)^{n/2} = 0$, and that the intergrid transfer operators are related by $I_H^h = (I_h^H)^T$, the 1×1 diagonal blocks of the Galerkin coarse grid operator A_H can shown to be equal to

$$A_H^\ell = (I_h^H)^\ell A_h^\ell (I_H^h)^\ell = \frac{2(1 - c_\ell^2) - \kappa^2(1 + c_\ell^2)}{2h^2} \tag{4.15}$$

for $1 \le \ell \le n/2 - 1$ and $(H_H)^{n/2} = 0$. For the eigenvalues of the coarse grid correction operator $P_{h,H}$ this implies that

$$\begin{aligned} P^\ell_{h,H} &= I - (I_H^h)^\ell (A_H^\ell)^{-1} (I_h^H)^\ell A_h^\ell \\ &= \begin{bmatrix} 1 - \frac{\frac{1}{2}(1 + \mathrm{c}_\ell)^2(-2 + 2\,\mathrm{c}_\ell + \kappa^2)}{2(\mathrm{c}_\ell^2 - 1) + \kappa^2(\mathrm{c}_\ell^2 + 1)} & \frac{\frac{1}{2}(\mathrm{c}_\ell^2 - 1)(2 + 2\,\mathrm{c}_\ell - \kappa^2)}{2(\mathrm{c}_\ell^2 - 1) + \kappa^2(\mathrm{c}_\ell^2 + 1)} \\ \frac{\frac{1}{2}(\mathrm{c}_\ell^2 - 1)(-2 + 2\,\mathrm{c}_\ell + \kappa^2)}{2(\mathrm{c}_\ell^2 - 1) + \kappa^2(\mathrm{c}_\ell^2 + 1)} & 1 + \frac{\frac{1}{2}(\mathrm{c}_\ell^2 - 1)(2 + 2\,\mathrm{c}_\ell - \kappa^2)}{2(\mathrm{c}_\ell^2 - 1) + \kappa^2(1 + \mathrm{c}_\ell^2)} \end{bmatrix} \end{aligned} \tag{4.16}$$

for $1 \le \ell \le n/2 - 1$ and $P^{n/2}_{h,H} = 0$. This real valued operator is a projection, and has 0 and 1 as eigenvalues.

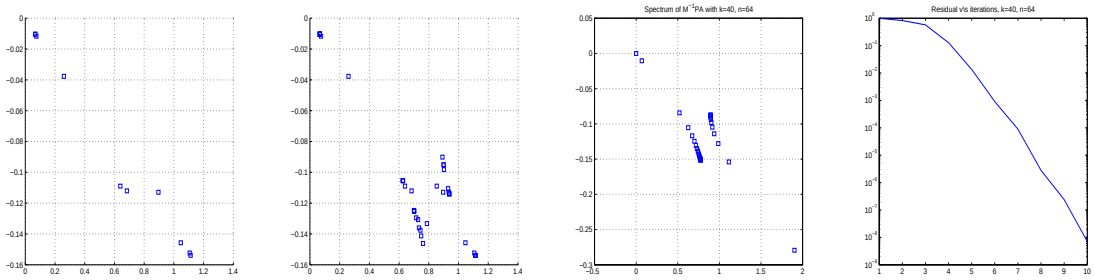

Figure 2: (From left) First two figures shows Ritz values of a Helmholtz problem with k=40, n=64 with Dirichlet boundary conditions, First figure shows the outlayer (away from cluster arround 1) are swept out with very first-few iterations, later ritz values converging to original spectrum. Right: Residual by GMRES, stagnation corresponding to first iterations is obvious.

4.3 Two Grid Analysis

Combining one pre-smoothing iteration of SLP with the coarse-grid correction operator, we arrive at the the two-grid operator

$$B_{h,H,(\beta_1,\beta_2)} = P_{h,H} S_{h,(\beta_1,\beta_2)} \,. \tag{4.17}$$

This operator has 0 as eigenvalue of multiplicity $n/2$ and $n/2-1$ eigenvalues of the form

$$\lambda^{\ell}(B_{h,H,(\beta_1,\beta_2)}) = \frac{a_\ell + \iota b_\ell}{c_\ell + \iota d_\ell} \tag{4.18}$$

where

$$\begin{aligned}
a_\ell &= (\beta_2^2\,\mathrm{c}_\ell^2 + \beta_2^2 - \beta_1^2 + \mathrm{c}_\ell^2\beta_1 + \beta_1 - \beta_1^2\,\mathrm{c}_\ell^2)\kappa^6 + (2\,\mathrm{c}_\ell^2 - 2 + 2\beta_1^2 - 2\,\mathrm{c}_\ell^2\beta_1^2 + 2\beta_2^2\,\mathrm{c}_\ell^2)\kappa^4 \\
&\quad +(4 - 4\beta_1 - 8\,\mathrm{c}_\ell^2 + 4\,\mathrm{c}_\ell^4 + 8\beta_1\,\mathrm{c}_\ell^2 - 4\beta_1\,\mathrm{c}_\ell^4)\kappa^2 \\
b_\ell &= (2\beta_1\beta_2 - \beta_2 - \mathrm{c}_\ell^2\beta_2 + 2\beta_1\,\mathrm{c}_\ell^2\beta_2 - \beta_1^2\,\mathrm{c}_\ell^2)\kappa^6 + (4\beta_1\,\mathrm{c}_\ell^2\beta_2 - 4\beta_1\beta_2)\kappa^4 \\
&\quad +(4\beta_2 - 8\,\mathrm{c}_\ell^2\beta_2 + 4\beta_2\,\mathrm{c}_\ell^4)\kappa^2 \\
c_\ell &= (\beta_2^2 - \beta_1^2 + \beta_2^2\,\mathrm{c}_\ell^2)\kappa^6 + (4\,\mathrm{c}_\ell^2\beta_1 + 2\beta_1^2 - 2\beta_2^2 + 4\beta_1 - 2\beta_1^2\,\mathrm{c}_\ell^2 + 2\beta_2^2\,\mathrm{c}_\ell^2)\kappa^4 \\
&\quad +(8\,\mathrm{c}_\ell^2\beta_1 - 4 - 8\beta_1 + 4\,\mathrm{c}_\ell^4)\kappa^2 + (8\,\mathrm{c}_\ell^4 - 16\,\mathrm{c}_\ell^2 + 8) \\
d_\ell &= (2\beta_1\beta_2 + 2\beta_1\beta_2\,\mathrm{c}_\ell^2)\kappa^6 + (4\beta_1\,\mathrm{c}_\ell^2\beta_2 - 4\beta_1\beta_2 - 4\beta_2 - 4\,\mathrm{c}_\ell^2\beta_2)\kappa^4 + (8\beta_2 - 8\,\mathrm{c}_\ell^2\beta_2)\kappa^2
\end{aligned}$$

In Figure (4.3) we plotted this spectrum setting $(\beta_1, \beta_2) = (1, .5)$ and for $k = 40$ and $n = 64$. These figures show that the spectrum consists of a cluster close to $(1, 0)$ surrounded by outliers. This spectrum is favorable for the convergence of GMRES, as outlayers are captured in the first iterations.

5 Numerical experiments

In this section we perform numerical experiments on the constant and non-constant wavenumber problems described in Section 2 and show that our solver is indeed scalable. It is obviously seen that moving of complex shift β_2 to zero lead to optimized preconditioner. As complex shift brings the damping, making preconditioner favorable for multigrid solve. By increasing complex shift, SLP more differ from original operator. Interestingly, this does not affect on deflation, which is

depicted in Figure(3). However in our experiments we use the shifts $(\beta_1, \beta_2) = (1, .5)$ unless stated differently. Both the shifted Laplace preconditioner and coarse grid linear system are solved using a direct method. The GMRES iterations are terminated if the scaled residual satisfies the relation

$$\frac{\|b_h - A_h x\|_2}{\|b_h\|_2} \leq 10^{-7}\,. \tag{5.1}$$

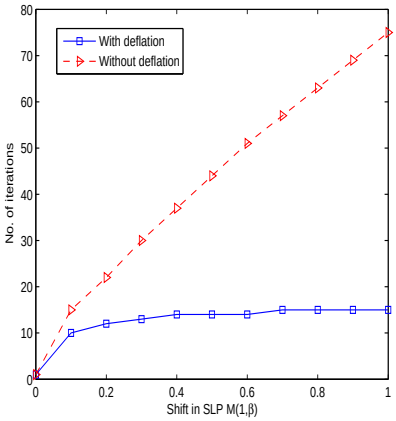

Figure 3: Number of iterations against the variation in complex shift β_2 for the constant wavenumber problem with $k = 50$ and $n = 80$

5.1 Constant Wavenumber Problem

We first consider the 2D constant wavenumber problem with Sommerfeld boundary conditions. In Figure 4 we show the spectrum of the smoother (or preconditioned operator) $S_{h,(1,.5)} = I_h - (M_{h,(1,.5)})^{-1} H_h$ and of two-grid (or deflated preconditioned) operator $B_{h,H} = P_{h,H} S_{h(1,.5)}$ with $k = 50$ and $n = 80$. This figure shows how the coarse grid correction transform the spectrum to a cluster of eigenvalues near 1 and and eigenvalue 0, rendering the deflated preconditioned problem easy to solve by GMRES. The comparison of this figure with similar pictures in the previous section shows that the problem with Sommerfeld boundary conditions is easier to solve than with Dirichlet boundary conditions. This is in agreement with earlier findings. Further this is guaranteed by comparison of two Tables (5.1 and 5.1) of Sommerfeld problem and Dirichlet problem, being the most intractable.

In Table 5.1 we give the required number of GMRES iterations required to solve the problem for a range of wavenumbers and mesh sizes. We require that the mesh is sufficiently fine to resolve the wavenumber given. The number of iterations for fixed k decreases with increasing n is likely due to be due to the use of the direct solver. For increasing n the coarse grid problem becomes larger, and our solver resembles more direct solver closer. In this preliminary work however we focuss on the number of iterations. In future work we will investigate the use of approximate solves for inverting the smoother and the coarse grid correction operator. We compare our solver with and without the use of deflation, making the effect of the deflation evident. Indeed, while without the use of deflation the iteration count depends on the mesh size, this is clearly no longer the case if deflation is used, which can apparently be seen by reading diagonal of the table. This table therefore proofs the fact that our solver in indeed scalable.

	$k = 10$	$k = 20$	$k = 30$	$k = 40$	$k = 50$	$k = 100$
$n = 18$	**5/9**	12/18	26/31	30/35	25/28	5/5
$n = 36$	4/10	**7/17**	14/30	34/50	53/73	60/66
$n = 50$	3/10	6/17	**11/30**	23/48	36/66	Singular Matrix*
$n = 64$	3/10	6/17	10/30	**17/47**	24/63	221/252
$n = 80$	3/10	5/17	7/30	13/46	**20/62**	251/229
$n = 160$	3/10	4/17	5/30	8/45	9/62	65/194
$n = 320$	2/10	3/17	4/30	5/45	6/61	**24/193**

Table 1: Number of GMRES iterations for the constant wavenumber problem with Dirichlet boundary conditions for different wavenumbers and grid resolutions using the preconditioner $S_{h,(1,.5)}$ with / without deflation.

	$k = 10$	$k = 20$	$k = 30$	$k = 40$	$k = 50$	$k = 100$
$n = 18$	**6/10**	12/17	27/36	40/49	29/30	5/5
$n = 36$	4/10	**7/17**	12/28	21/41	39/63	66/67
$n = 50$	4/10	6/17	**10/28**	15/38	23/48	396/419
$n = 64$	4/10	6/17	8/28	**12/36**	18/45	173/163
$n = 80$	4/10	5/17	7/27	10/35	**14/44**	156/116
$n = 160$	3/10	4/17	5/27	6/35	8/43	25/82
$n = 320$	3/10	4/17	4/27	5/35	5/42	**10/80**

Table 2: Number of GMRES iterations for the constant wavenumber problem with Sommerfeld boundary conditions for different wavenumbers and grid resolutions using the preconditioner $S_{h,(1,.5)}$ with / without deflation.

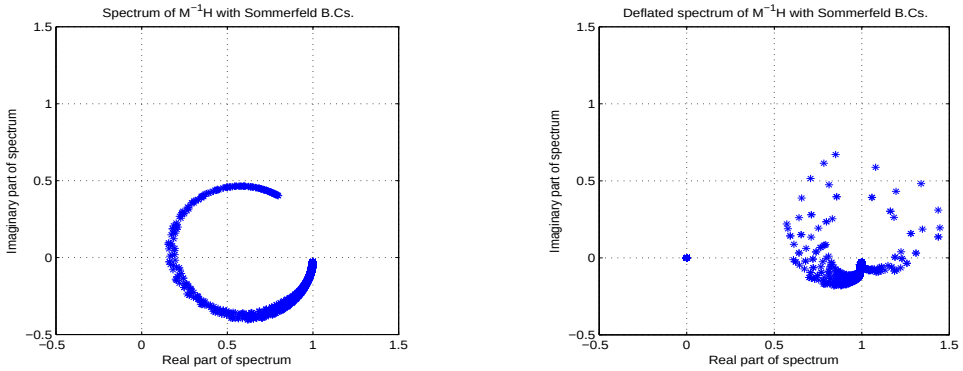

Figure 4: Spectrum of 2-D Helmholtz operator preconditioned with $M(1, 0.5)$ with k=50 and $n = 80$ with (left) and without (right) deflation.

5.2 Non Constant Wavenumber Problem

Next we consider the non-constant wavenumber problem. As in the previous example, we give in Table 5.2 the required number of GMRES iterations for different wavenumbers and mesh sizes with and without deflation. This table shows that even in the case of constast in the wave number our solver remains scalable.

	$freq = 10$	$freq = 20$	$freq = 30$	$freq = 40$	$freq = 50$
74×124	**7/33**	20/60	79/95	267/156	490/292
148×248	5/33	**9/57**	17/83	42/112	105/144
232×386	5/33	7/57	**10/81**	25/108	18/129
300×500	4/33	6/57	8/81	**12/105**	18/129
374×624	4/33	5/57	7/80	9/104	**13/128**

Table 3: Number of GMRES iterations for the non-constant wavenumber problem for different wavenumbers and grid resolutions using the preconditioner $S_{h,(1,.5)}$ with / without deflation.

6 Conclusions

We have studied scalable solver for the discrete Helmholtz equation by combining the shifted Laplace preconditioner with multigrid deflation. We theoretically analysed our scheme by Fourier analysis, for Dirichlet boundary conditions, being the worst case. Numerical results support this analysis and confirms that the number of iterations is frequency independent.

References

[1] C. G. A. Bayliss and E. Turkel. An iterative method for the Helmholtz equation. *Journal of Computational Physics*, 49:443 – 457, 1983.

[2] T. Airaksinen, E. Heikkola, A. Pennanen, and J. Toivanen. An algebraic multigrid based shifted-Laplacian preconditioner for the Helmholtz equation. *Journal of Computational Physics*, 226(1):1196 – 1210, 2007.

[3] M. Bollhöfer, M. J. Grote, and O. Schenk. Algebraic multilevel preconditioner for the Helmholtz equation in heterogeneous media. *SIAM Journal on Scientific Computing*, 31(5):3781–3805, 2009.

[4] M. Eiermann, O. Ernst, and O. Schneider. Analysis of acceleration strategies for restarted minimal residual methods. *J. Comput. Appl. Math.*, 123(1-2):261–292, 2000.

[5] Y. Erlangga. *A robust and effecient iterative method for numerical solution of Helmholtz equation.* PhD thesis, DIAM, TU Delft, 2005.

[6] Y. Erlangga and R. Nabben. On a multilevel krylov method for the helmholtz equation preconditioned by shifted laplacian.

[7] Y. Erlangga and R. Nabben. Multilevel projection-based nested krylov iteration for boundary value problems. *SIAM J. Sci. Comput.*, 30(3):1572–1595, 2008.

[8] Y. A. Erlangga and R. Nabben. Deflation and balancing preconditioners for krylov subspace methods applied to nonsymmetric matrices. *SIAM J. Matrix Anal. Appl.*, 30(2):684–699, 2008.

[9] Y. A. Erlangga, C. W. Oosterlee, and C. Vuik. A novel multigrid based preconditioner for heterogeneous Helmholtz problems. *SIAM J. Sci. Comput*, 27:1471–1492, 2006.

[10] J. Frank and C. Vuik. On the construction of deflation-based preconditioners. *SIAM J. Sci. Comp.*, 23:442–462, 2001.

[11] L. Giraud, S. Gratton, X. Pinel, and X. Vasseur. Flexible gmres with deflated restarting. *SIAM Journal on Scientific Computing*, 32(4):1858–1878, 2010.

[12] A. Laird. Preconditioned iterative solution of 2d helmholtz equation. Technical report, St. Hugh's college, 2001.

[13] R. B. Morgan. A restarted GMRES method augmented with eigenvectors. *SIAM J. Matrix Anal. Appl.*, 16(4):1154–1171, 1995.

[14] R. B. Morgan. Gmres with deflated restarting. *SIAM J. Sci. Comput.*, 24(1):20–37, 2002.

[15] R. A. Nicolaides. Deflation of conjugate gradients with applications to boundary value problems. *SIAM J. Numer. Anal.*, 24(2):355–365, 1987.

[16] R. E. Plessix and W. A. Mulder. Separation-of-variables as a preconditioner for an iterative Helmholtz solver. *Appl. Numer. Math.*, 44:385–400, 2003.

[17] J. M. Tang. *Two Level Preconditioned Conjugate Gradient Methods with Applications to Bubbly Flow Problems.* PhD thesis, DIAM, TU Delft, 2008.

[18] U. Trottenberg, C. W. Oosterlee, and A. Schüller. *Multigrid.* Academic Press, London, 2000.